ELSEVIER

International Journal of Mass Spectrometry 190/191 (1999) 103–111

International Journal of Mass Spectrometry

Mass selective instability mode without a light buffer gas

Ernst P. Sheretov*, Oleg W. Rozhkov, Dmitri W. Kiryushin, Alexander E. Malutin

Department of Physics, Ryazan State Radio Technical University, Ryazan 391000, Russia

Received 22 September 1998; accepted 15 December 1998

Abstract

The mass selective axial instability mode without a light buffer gas for a three dimensional ion trap was investigated. This technique is different from the well-known "mass selective axial instability mode" and based on radial injection of an ionizing electron beam into the analyzer without a light buffer gas. The influence of the axial dimensions of the ionization region, the range of initial phase of ionization, and the scan speed on the features of the analyzer is obtained from the numerical simulations. It is shown that the presence of a light buffer gas decreases the maximum resolution that can be achieved in this mode. We present here experimental results and mass spectra of different organic compounds obtained with the ion trap operated in the mass selective instability mode without a light buffer gas. (Int J Mass Spectrom 190/191 (1999) 103–111)

Keywords: Quadrupole ion trap; Mass spectrometry; Mass selective axial instability; Buffer gas; Radial electron injection

1. Introduction

Since 1990 ion traps have become the most popular mass detectors for gas chromatography [1] and successfully compete with the previously dominant quadrupole mass filters [2]. This was first caused by a new operational mode called the "mass selective axial instability mode" [3]. A great number of original works concerning the practical implementations of this mode and its improvements have been presented. A superlative review was published by March et al. [1,4].

All these publications describe mass spectrometers differing in design or operation modes, but the common base for all of them is an electrode system that consists of three hyperbolic electrodes: a ring and two endcaps. Injection of the ionizing electron beam is carried out along the longitudinal axis of the analyzer, and all devices operate in the presence of significant background pressure from a light buffer gas (up to 10^{-3} Torr) of helium that "cools" the kinetic energy of the analyzed particles. The first works have shown that a light buffer gas considerably improves analytical performance (i.e. resolution, sensitivity) of the ion trap operating in the mass selective axial instability mode [3,5].

From our point of view, a light buffer gas and axial injection of electron beam limit the parameters of ion traps and areas of their applications. This can be explained by the following factors: (1) the main working parameters of an analyzer (resolution and sensitivity) depend on the background pressure of the buffer gas and therefore, the helium pressure should be stabilized [5,6]; (2) sensitivity and dynamic range

* Corresponding author. E-mail: sheretov@eac.ryazan.su

Dedicated to J.F.J. Todd and R.E. March in recognition of their original contributions to quadrupole ion trap mass spectrometry.

1387-3806/99/$20.00
PII S1387-3806(99)14293-8

are limited by the space charge of the trapped ions, and the presence of helium buffer gas atoms with concentrations exceeding the concentration of particular components of the analyzed ions increases the problem; (3) axial injection of an electron beam requires a preliminary phase of collisional focusing of the ion cloud, which limits maximum mass scan rate.

The necessity of a light buffer gas in the case of the mass-selective axial instability mode is caused by features of the ionization process, and, in particular, by axial injection of the electron beam. The ions are formed with a large spread of initial coordinates along the *z* axis. In order to achieve high analytical performance they must be compressed to the electrode system center (the precursory stage of collisional cooling of the trapped ions) [5].

Another (radial) manner of ionizing electron beam injection has been reported [7–9]. We successfully used this technique for hyperboloid mass spectrometers in space exploration [10] and for other purposes [11].

For the ion trap operating in this manner, the injection of the ionizing electron beam is carried out through a hole or a narrow slit in the ring electrode. The center of this hole lies in the saddle point of the hyperboloid generating line. As a result, almost all the trapped ions are localized in the vicinity of the center, and have small initial *z* coordinates, so there is no necessity in the precursory stage for a collisional focusing of the trapped ions. Thus, the use of radial injection of the electron beam in the mass selective instability mode completely obviates the need for a light buffer gas.

2. Computer simulation of the mass selective instability mode without a light buffer gas

In order to estimate the effectiveness of this mode we have conducted computer simulations of the mass selective instability mode without a light buffer gas. For this purpose we studied the ion trap operated with a working pulse signal and a phase injection of an electron beam. A mass scan was performed by varying frequency. The rf signal is a sequence of impulses of different polarity with a given amplitude and duration. The following assumptions were made: (1) the electrode system of the ion trap is axially symmetric and consists of a ring and two endcap electrodes with a hyperbolic profile; characteristic dimensions of the electrode systems are r_a and d, where r_a is the minimum distance between the electrode system center and the ring electrode, and d is the minimum distance between the electrode system center and one endcap (in this case we take $r_a = d$); (2) the electric field within the analyzer is ideal; (3) the dimensions of the ionization region normalized to the characteristic dimensions r_a and d, respectively, were: (−1.0–1.0) along the *r* coordinate, and (−0.01–0.01) along the *z* coordinate; (4) all ions have uniform distribution of initial velocities within the range of mean-square thermal velocity corresponding to $T = 500$ K.

The region of initial localization was uniformly filled with a number of ions, a quantity of which was determined by a particular dynamic range. For each ion we calculated its trajectory and path length, taking into account the possible collisions. Trajectories of ions were defined by the Hill equation. A period of time between interactions depending on an ion energy was approximately determined either by a constant free path or a constant drift time (in the case of a polarization scattering). We also assumed that in the system of inertia center the scattering of interacting particles is isotropic. Scattering angles were taken randomly. Velocities of neutral molecules before each interaction were equal to the thermal ones; their directions were also taken randomly.

The simulations showed that a mass peak shape depends significantly on the background pressure of helium. This corresponds to the results that were reported by Goeringer et al. [12]. Mass peaks of *m/z* 200 Da for different background pressures of a light buffer gas with *m/z* 4 Da are presented in Fig. 1. The scan line corresponds to $a_i = 0$ (no dc voltage). The initial working point of the ions on the stability diagram was $q_i = 0.34$. This value of q_i corresponds to the working rf signal in the shape of rectangular pulses of different polarity. The edge of the stability boundary was $q_i = 0.356$ ($\beta_z = 1$). The values of parameters a_i and q_i correspond to parameters a and q

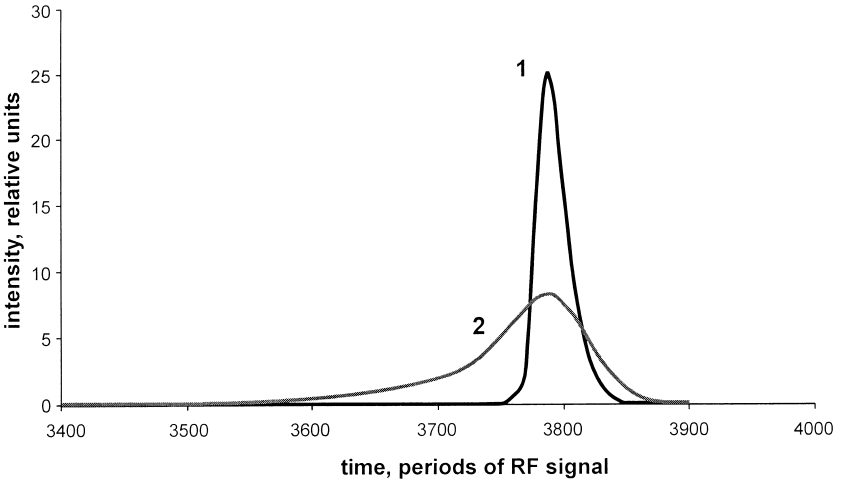

Fig. 1. Mass peak shape of *m/z* 200 Da as a function of background pressure of a light buffer gas (*m/z* 4 Da) obtained in the mass selective instability mode ($V_q = 2 \times 10^{-4}$): 1—helium pressure of 10^{-6} Torr; 2—helium pressure of 10^{-4} Torr.

in the Mathieu equation. For these new parameters the ac component $U_{\sim}$ of the working signal can be described in the following form:

$$U_{\sim} = (|\Delta U_1| + |\Delta U_2|)/2, \quad (1)$$

and the dc component $U_{=}$:

$$U_{=} = \frac{|\Delta U_1| t_1 - |\Delta U_2| t_2}{t_1 + t_2}, \quad (2)$$

where ΔU_1 and ΔU_2 are the potential differences between the ring and endcap electrodes during the positive and the negative pulses, respectively; and t_1 and t_2 are the positive pulse duration and the negative pulse duration, respectively. We use a signal with $t_1 = t_2$. We take $\Delta U_1 = \Delta U_2$ in order to fulfill the condition $a_i = 0$.

Ions were created around the optimal phase of the first kind for the *r* coordinate. This allows maximum amounts of ions to be stored. The optimal phase of the first kind is the phase of ion formation for which coordinates of the "stable" ions created with zero velocities do not exceed their initial coordinates within the confinement time (parameters of the rf field are kept constant). This phase corresponds to the middle of the pulse when ions are focused along the given coordinate. The middle of the opposite pulse (defocusing pulse) is the optimal phase of the second kind.

A mass scan was performed by discrete changing of the rf frequency. The frequency was changed every 16 periods with a specified step that defined the relative changing of the working point q_i ($V_q = \Delta q_i/q_i$) on the stability diagram. The buffer gas causes "diffusion" of the mass peak (Fig. 1), and, respectively, decreases mass resolution. We should remember that the calculation we have conducted implies that ions were created with small *z* coordinates within a narrow region close to the origin. This important result can be illustrated by the data presented in Table 1. The third column of this table corresponds to the peaks presented in Fig. 1. It can be seen from Table 1 that the influence of the buffer gas on mass resolution is different for different scan speed. For the scan speed $V_q = 2 \times 10^{-4}$ and the helium pressure of 10^{-6} Torr, a resolution of 3846 was achieved; and for

Table 1
Resolution defined at level 0.5 from a peak height as a function of the helium pressure for different values of V_q

Pressure, Torr	Resolution $R_{0.5}$, relative units		
	$V_q = 1.6 \times 10^{-2}$	$V_q = 8 \times 10^{-4}$	$V_q = 2 \times 10^{-4}$
10^{-6}	143	833	3846
10^{-5}	125	500	1667
10^{-4}	111	392	1250
10^{-3}	111	339	192

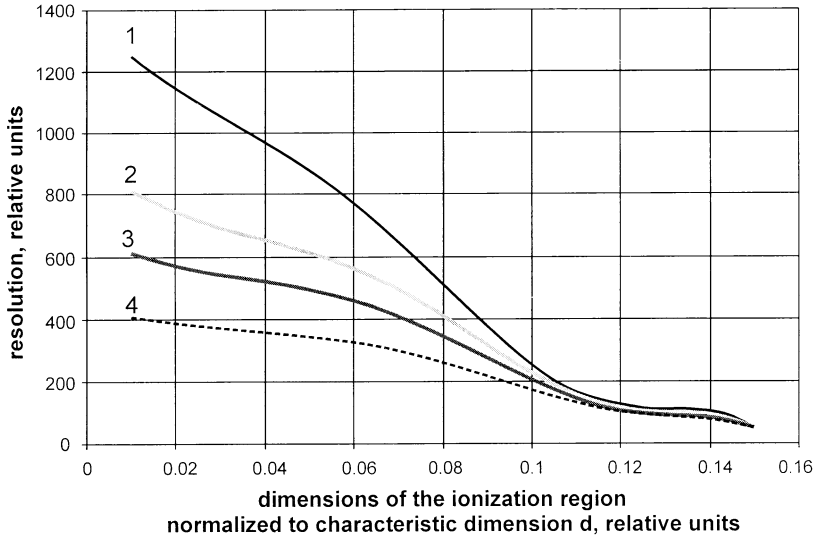

Fig. 2. The dependence of resolution on axial dimensions of the ionization region (normalized to the axial dimension d of the ion trap) for ionization during the optimal phase of the first kind. Resolution was defined at the following levels: 1—at level 10^{-1}; 2—at level 10^{-2}; 3—at level 10^{-3}; 4—at level 10^{-6}.

the pressure of 10^{-3} Torr, resolution was about 10 times less. At the same time, when the buffer gas pressure is increased by the same value for the scan speed $V_q = 1.6 \times 10^{-2}$ resolution is decreased by 22% only. We note, however, that maximum resolution is decreased (from 3846 to 143). Thus, it follows from the obtained simulation results that there is a possibility to implement the mass selective instability mode without a light buffer gas.

One of the basic problems was to define ionization region dimensions that give the needed resolution for a given working point, an ionization phase, and a scan speed. The values of mass resolution at varying levels from 10^{-1}–10^{-6} were defined. Resolution as a function of axial dimension of the ionization region is shown in Fig. 2. The ionizing electron beam was injected during the optimal phase of the first kind for the r coordinate. We see that the broadening of the ionizing electron beam sharply decreases resolution. This requires one to design an electron source forming a very narrow beam with minimal thickness in the z direction.

The values of resolution at levels from 10^{-1}–10^{-6} as a function of different ionization phase are demonstrated in Fig. 3 for a constant electron beam thickness ($0.01d$). Maximum points of these functions correspond to the optimal phases of the first and the second kinds. Small drift of a maximum point from the middle of pulses can be explained by the phase features of ion trajectories. When we take integral dependence of resolution on ionization pulse duration we obtain a matching of the maximum point and the middle of ionization pulse that, in turn, corresponds to the optimal phase of the first kind for the r coordinate (Fig. 4).

In the mass selective instability mode, resolution depends on the velocity of the working point approaching to the “separation” boundary. Therefore, in order to achieve the needed resolution it is very important to define the appropriate ejection/detection speed.

In the case when mass scan is carried out by changing the frequency f, it is necessary to define the dependence of a relative change of the frequency $\Delta f/f$ and the period of its changing N_c on the mass of the detected ions M. This value of M determines the minimal allowed resolution R. The value of N_c is defined in periods of the rf field.

In order to investigate the influence of the scan speed on resolution in the mass selective instability mode without a light buffer gas we calculated resolution $R_{0.1}$ (resolution at the level of 0.1 from a peak

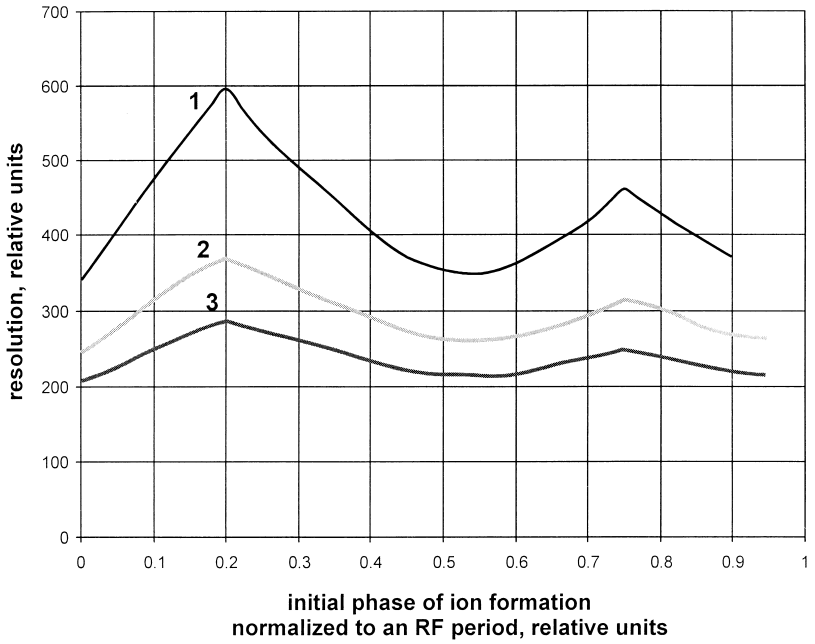

Fig. 3. The dependence of resolution on initial phase of ion formation. Resolution was defined at the following levels: 1—at level 10^{-1}; 2—at level 10^{-2}; 3—at level 10^{-3}.

height) for different initial working points on the scan line $a_i = 0$. From the conducted simulations we defined the dependence of the resolution $R_{0.1}$ on the relative change of the frequency $\Delta f/f$ for a constant value of N_c. We have found that this dependence can be described in the following form:

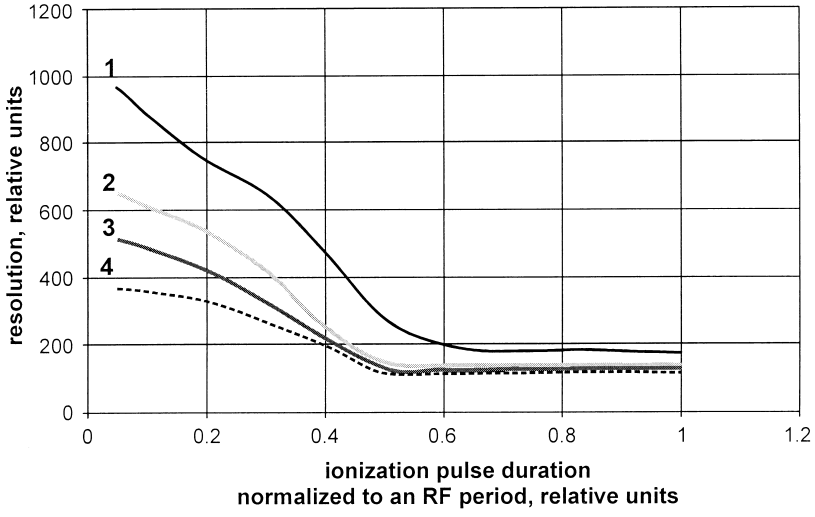

Fig. 4. The dependence of resolution on ionization pulse duration: 1—resolution at level 10^{-1}; 2—resolution at level 10^{-2}; 3—resolution at level 10^{-3}; 4—resolution at level 10^{-6}.

Table 2
The sorting time and the average scan speed calculated from Eq. (3)

	Mass range, Da	Sorting time, μs	Average scan speed, Da s^{-1}
1	10–30	423.6	47 169
2	30–90	3446.1	17 411
3	90–270	31362.3	5740
4	270–700	206606.8	2081

$$\frac{\Delta f}{f N_c} = \frac{C}{M^p} \tag{3}$$

where M is the ion mass corresponding to the working point lying on the boundary of the stability diagram and defining the needed resolution $R_{0.1} = 1M$; and C and p are coefficients. In the case when ions are created by the ionizing electron beam ($0.01d$ thick) during the optimal phase of the first kind for the r coordinate the values of coefficients C and p are equal to 0.57 and 1.5385, respectively.

From Eq. (3) we can obtain an average scan speed, frequency, and an average sorting time. The values of these parameters for the frequency range (0.0965–0.8225) MHz, the rf voltage of 400 V peak to peak, electrode system dimensions $r_a = d = 19$ mm, mass range of (10–700) Da, and scan line location $a_i/q_i = 0$ are presented in Table 2. The total scan time for the whole mass spectrum of (10–700) Da is 0.241 s, and the average scan speed is 2903 Da s^{-1}.

It follows from the simulations by using Eq. (3) that in the mass selective instability mode without the buffer gas the needed resolution (up to $R_{0.1} = 800$) can be achieved when the rf signal with a small dc potential (positive or negative) is applied to the electrodes. This small dc potential changes the value of ratio a_i/q_i by only ± 0.1.

3. Experimental study of the mass selective instability mode without a light buffer gas

Experimental investigation of the mass selective instability mode without a buffer gas was carried out by using the ion trap, the electrode system of which is shown in Fig. 5 ($d = r_a = 19$ mm). The ionizing

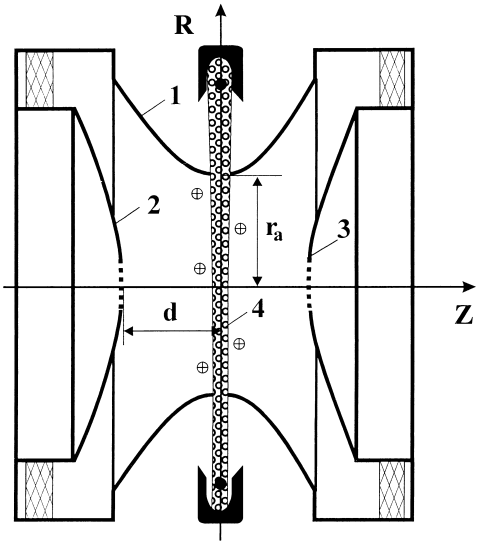

Fig. 5. Electrode system of the ion trap with radial injection of the ionizing electron beam: 1—the ring electrode; 2, 3—the endcap electrodes; 4—the ionizing electron beam.

electron beam was injected through the 0.3 mm thick ($0.008d$ thick) narrow slit in the ring electrode. The sorted ions were ejected through a shaped grid (with transparency of 40% and radius of $0.5r_a$) in one of the endcaps. A vacuum chamber was pumped with a 160 L/min turbomolecular pump. The vacuum chamber and the electrode system were heated to 200 °C.

An rf pulse of 400 V peak to peak (positive polarity) with pulse period-to-pulse duration ratio of 2 was applied to the endcap electrodes, and a constant voltage changing from 180–250 V was applied to the ring electrode. Operation of the ion trap without a dc potential ($a_i = 0$) corresponds to a constant voltage of 200 V applied to the ring electrode.

The potential of the ring electrode used in the experiment was slightly less than 200 V. This small negative potential bias corresponds to the value of $a_i/q_i = 0.1$ and does not affect the peak shape, but decreases the noise content considerably. Besides, it follows from the conducted simulations that operational parameters of the ion trap with a small dc potential in the mass selective instability mode without a buffer gas corresponds to the parameters of the ion trap without any dc potential. This allows one to

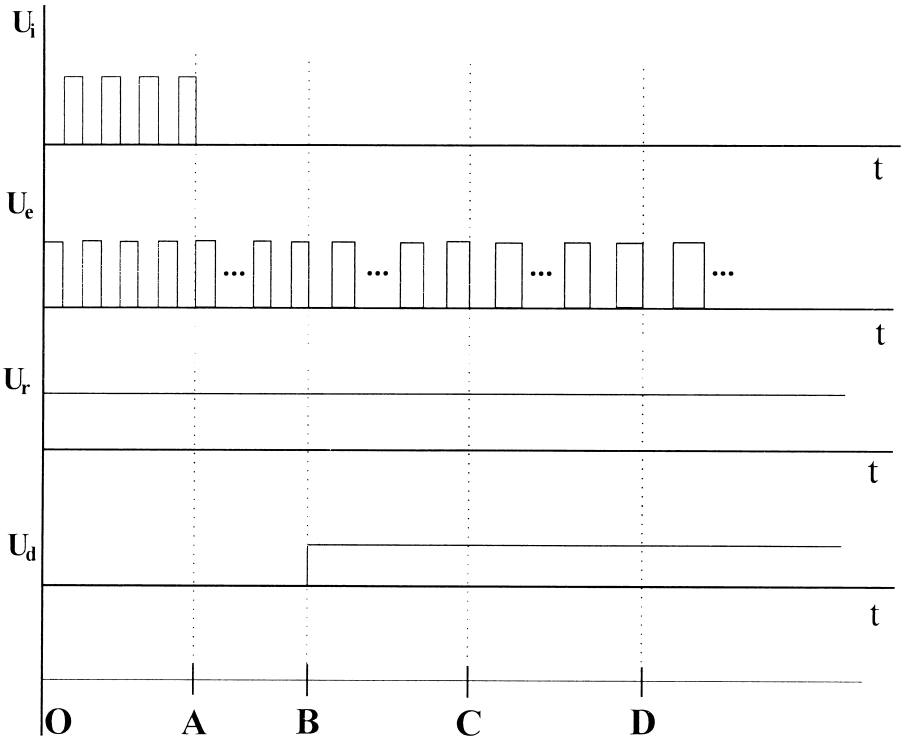

Fig. 6. Timing sequence for the operation of the ion trap in the mass selective instability mode without a light buffer gas.

compare the results obtained from experiments and simulations.

The timing sequence for the operation of the ion trap in the mass selective instability mode is shown in Fig. 6, where U_i is the ionization pulse, U_e is the potential of the endcap electrodes, U_r is the potential of the ring electrode, and U_d is a detection system driving voltage. Ionization of the analyzed particles was performed by four pulses (O-A interval of the scan function). The duration of each pulse is equal to half of an rf period. The potential of the endcaps was negative relative to the potential of the ring electrode. This ensured additional electron beam compression towards the electrode system center. The frequency of the working signal was chosen so that the ion trap confined ions within a little more than the previously defined mass range. At the end of the ionization process there was no "collisional cooling" stage of the trapped ions before the mass selective ion ejection began. A mass scan was performed by changing the frequency of the rf signal every 16 periods (A-B, B-C, C-D steps, etc.). The output ion signal was read before the frequency changing. In order to prevent axially unstable ions of low mass with a mass different from the preset mass-to-charge ratio from being registered, the gating of the detection system was delayed (A-B step).

Experimental results of the mass selective instability mode without a buffer gas are presented in Fig. 7 and 8. A part of the mass spectrum obtained in the mass selective instability mode without a light buffer gas in the case working volume is filled with an acetone-benzene-toluene mixture in the proportion 1:1:1 under the pressure of 10^{-5} Torr as shown in Fig. 7.

The sample pressure was varied in the range from 10^{-7}–10^{-4} Torr in experiments. It follows from the experimental and simulation results that the maximum working pressure is about 5×10^{-5} Torr. When the sample pressure is greater than this value interactions

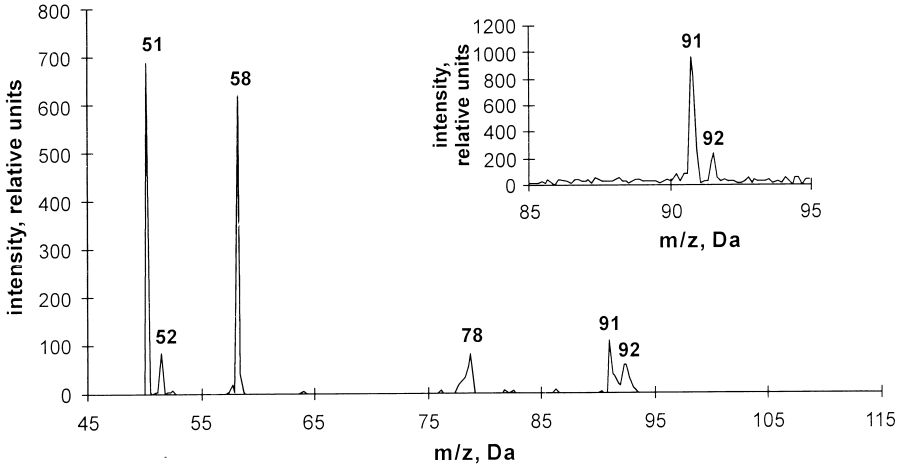

Fig. 7. A mass spectrum obtained from head space analysis of an acetone–benzene–toluene mixture for the mass selective instability mode without a buffer gas.

between the analyzed ions and neutral particles of the sample are increased and this causes the ion scattering to increase ("self-divergence").

Electron impact ionization was used for the formation of ions. Emission current was 20 μA, and electron energy varied from 85 eV in the electrode system center (small *r* coordinates) to 150 eV near the ring electrode. The mass scan within the mass range of (40–120) Da was performed by changing the frequency corresponding to a 0.2 Da step. The average scan speed was 2000 Da s^{-1}. In the upright corner of Fig. 7 a part of the mass spectrum containing characteristic toluene peaks (*m/z* 91 and 92 Da) taken under the same condition with a 0.1 Da step is shown.

The working parameters of both modes with and without helium in the ion trap were compared according to characteristic peaks of the carbon tetrachloride (CCl_4) spectrum corresponding to the ions *m/z* 117, 119, and 121 Da. Spectra areas taken in the mass selective instability mode with the same analyzer without and with helium within an hour interval are presented in Fig. 8(a) and (b), respectively. In the

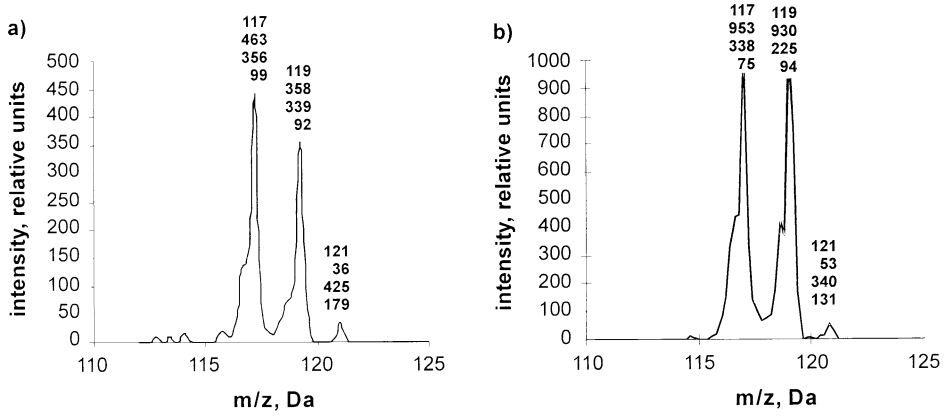

Fig. 8. Characteristic peaks of carbon tetrachloride (CCl_4) obtained in the mass selective instability mode for radial electron beam injection: a) without helium; and b) in the presence of helium under a pressure of 10^{-4} Torr.

former case the helium pressure was 10^{-4} Torr. The dc voltage applied to the ring electrode was maintained at 188 V. Four numbers located near the mass peaks represent ion mass, relative signal intensity, and resolution defined at the levels 0.5 and 0.1 from a peak height, respectively.

The obtained results show that in both cases resolution does not depend on presence or absence of the buffer gas. From our point of view it is connected with high scan speed $V_q \approx 2 \times 10^{-3}$. This corresponds to Table 1, from which it is clear that scan speed increase leads to reduction of the light buffer gas effect on the resolution. As for signal intensity, the helium injection increases it twice. We believe that this is caused by a collisional compression of the ion cloud to the electrode system center in the radial direction, and it results in a decrease in the number of ions lost during ejection through the endcap electrode, which is very important in determining the method of introducing electrons for ionization to be used.

4. Conclusions

The obtained experimental results and the computer simulation results described above show that ion traps can operate in the mass selective instability mode without a buffer gas with radial injection of the ionizing electron beam. In some cases, despite a certain loss of sensitivity, this version simplifies design and lowers weight and overall dimensions of mass spectrometers and has good prospects for practical use.

We hope that the results presented will be helpful for researchers who develop mass analyzers based on the ion trap and for ion trap users as well.

References

[1] R.E. March, Mass Spectrom. 32 (1997) 351.
[2] M.A. Grayson, J. Chromatography Sci. 24 (1986) 529.
[3] G.C. Stafford, P.E. Kelley, D.R. Stephens, U.S. Patent N4540884, 1985.
[4] R.E. March, R.J. Hughes, Quadrupole Ion Storage Mass Spectrometry, Wiley Interscience, New York, 1989.
[5] G.C. Stafford, P.E. Kelley, J.E.P. Syka, W.E. Reynolds, J.F.J. Todd, Int. J. Mass Spectrom. Ion Processes 60 (1984) 85.
[6] D.W. Kiryushin, The influence of a light buffer gas on ion-confinement within the ion trap (Book of papers), Ryazan State Radio Technical University, Ryazan, 1997, p. 123.
[7] C.S. Harden, P.E. Wagner, Three Dimensional Quadrupole Mass Analyser. I. General Description, Edgewood Arsenal Special Publications, Unclassified Report (1971) p. 100.
[8] C.S. Harden, P.E. Wagner, A Three Dimensional Quadrupole Mass Analyser. II. Operational Characteristics, Edgewood Arsenal Technical Report 4545, 1971, p. 7.
[9] E.P. Sheretov, B.I. Kolotilin, V.F. Samodurov, Hyperboloid Ion Trap Mass Spectrometer, Inv. Cert. SU 1103301A, 26, 1984.
[10] Y.A. Surkov, W.F. Ivanova, A.N. Pudov, W.P. Wolkov, E.P. Sheretov, B.I. Kolotilin, M.P. Safonov, R. Toma, G. Lespangnol, Lett. J. Astron. 12 (1986) 110.
[11] E.P. Sheretov, B.I. Kolotilin, O.W. Rozhkov, E.W. Mamontov, N.V. Vesyolkin, S.P. Ovchtinnikov, A.E. Malutin, Conversion 6 (1996) 15.
[12] D.E. Goeringer, W.B. Whitten, J.M. Ramsey, S.A. McLuckey, G.L. Glish, Anal. Chem. 64 (1992) 1432.